AeroBest 2021

International Conference on Multidisciplinary Design Optimization of Aerospace Systems

Proceedings

21–23 July 2021
Lisboa, Portugal

André C. Marta & Afzal Suleman (editors)

Published by:
IDMEC
Instituto Superior Técnico
Universidade de Lisboa
Portugal
https://aerobest2021.idmec.tecnico.ulisboa.pt/

ISBN: 978-989-99424-8-6

Editors:
André C. Marta
Afzal Suleman

AeroBest 2021
Lisboa, 21-23 July 2021

ADAPTIVE MORPHING OF TENSEGRITY-BASED HELIUM-FILLED AEROSTATS

Lech Knap[1], Andrzej Świercz[2*], Cezary Graczykowski[2], Jan Holnicki-Szulc[2]

1: Institute of Vehicles and Construction Machinery
Warsaw University of Technology
Narbutta 84, 02-524 Warsaw, Poland
Lech.Knap@pw.edu.pl, http://www.simr.pw.edu.pl

2: Institute of Fundamental Technological Research
Polish Academy of Sciences
Pawinskiego 5B, 02-106 Warsaw, Poland
{aswiercz, cgraczyk, holnicki}@ ippt.pan.pl, http://www.ippt.pan.pl

Abstract *In this contribution the authors propose and investigate the concept of adaptive morphing for recently introduced tensegrity-based helium-filled aerostats. The proposed aerostat is based on an ultra-light tensegrity structure equipped with prestressed tensioned elements of controllable lengths. Such internal structure allows for adaptive morphing of the aerostat defined as simultaneous controllable modifications of aerostat volume and external shape during the flight. The controlled volume changes enable influencing buoyancy forces acting on the envelope and obtaining desired vertical motion of the aerostat during the ascending and descending process ("vertical mobility"). In turn, the controlled changes of external shape of the aerostat can be used either for lowering the aerodynamic drag forces and reducing energy usage needed to maintain stable horizontal position or to follow the desired path of aerostat horizontal motion ("horizontal stability"). The authors effectively apply the previously introduced mechanical FEM model of the tensegrity-based aerostat and dynamic model of the aerostat's vertical and horizontal motion to conduct simulations of the process of adaptive morphing and maintain a proper position in the atmosphere. The obtained results positively verify the idea of adaptive morphing and its efficiency in controlling vertical and horizontal motion of the aerostat.*

Keywords: tensegrity structure, helium-filled aerostat, adaptive morphing, vertical mobility, horizontal stability

1. INTRODUCTION

The airships and balloons were the first vehicles built by men and although their use was originally widespread, they have been superseded for many years by aircrafts. In recent years it has been observed a renewed interest in aerostats, mainly due to their ability to carry out long missions at much lower costs than aircrafts [1]. Currently constructed airships successfully fulfil various purposes, e.g. provide communication in hardly reachable areas (including ensuring the possibility of using 4G / 5G technology), serve as reconnaissance and surveillance systems, military communication centres or research pseudo-satellites [2]. For example, stratospheric airships offer adequate operational flexibility, which allow to provide locally broadband telecommunications and connectivity in areas of natural disasters or areas with a low level of ground infrastructure in much faster and easier way [3]. Simultaneously, the total costs (mainly consisting of fuel and service) for cargo transport or for exploration of stratosphere, mesosphere – and even space observation – are much lower than in case of using airplanes or satellites [1,4-5].

Although air vehicles are more and more used, their wider application is still limited by a number of design problems. These mainly include adequate structural strength, which must be ensured at the lowest possible weight. Increase of the structure self-weight causes that the possible payload diminishes. Therefore, the significant effort in design and construction of the airships is oriented towards reduction of the self-weight by reducing mass of internal structure and mass of the envelope. The main technological challenge is to develop ultra-light envelopes (range 2.8-24 μm), which are impermeable to helium, resistant to UV radiation and maintain elastic properties at temperatures reaching -70°C [6-7]. The problem is to ensure that the internal structure is sufficiently stiff to provide the adequate shape and volume necessary for the airship to fly with a designed payload and under the load exerted by the wind flow.

Currently, many research works are devoted to solving problem of predicting the movement of airships in both the vertical and the horizontal direction [8-9], as well as to analyse the changes in volume resulting from heating of the envelope by the sun and heat exchange with the environment [10-11].

In this article the authors propose and investigate the concept of adaptive morphing for recently introduced tensegrity-based helium-filled aerostats. The proposed aerostat is based on an ultra-light tensegrity structure equipped with prestressed tensioned elements of controllable lengths. Such internal structure allows for adaptive morphing of the aerostat defined as simultaneous controllable modifications of aerostat volume and external shape during the flight. The controlled volume changes enable influencing buoyancy forces acting on the envelope and obtaining desired vertical motion of the aerostat during the ascending and descending process ("vertical mobility"). Additionally, the controlled changes of the altitude can be used to maintain horizontal position in appropriate weather conditions.

The proposed internal structure of the aerostat is based on the use of tensegrity type construction. Such a construction allows to obtain a relatively low mass of the internal structure but also provides adequate strength of the aerostat. An additional advantage of such a structure is the possibility to control its selected elements (e.g. shortening of tendons or elongation of struts), which enables to obtain various shapes of the envelope stretched on the structure. In this way it is possible to control the aerostat balloon volume within a certain range. With an appropriate configuration of the tensegrity structure, the aerostat can be assembled and transported using different means of transport e.g., a rocket or an aircraft. In this way the adaptive aerostat can be delivered quickly to a chosen point of the atmosphere and disassembled.

2. CONCEPT OF THE ADAPTIVE AEROSTAT

An example of application of supporting lightweight truss structure with modifiable lengths of selected members used to reinforce the helium-filled aerostat is demonstrated in a simplified form in Fig.1. For the clarity of the presented approach, the further discussed vertical mobility problem is presented using 2D model.

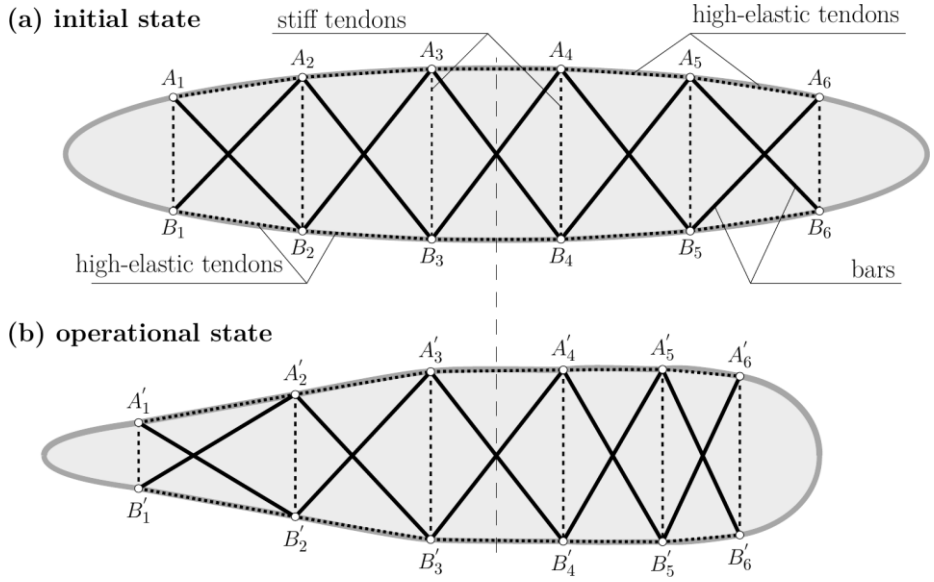

Figure 1. Aerostat reinforced by the lightweight truss supporting structure: (a) initial state with designed element lengths; (b) operational state – after possible modification of controllable members lengths.

The internal truss structure is composed of 5 sections and each section consists of 3 types of elements: rigid bars (diagonal members), high-elastic tendons (top and bottom members) and stiff tendons (vertical members). The nodal points of the initial supporting structure are denoted by A_i (top members) and B_i (bottom members), see Fig.1a. Lengths modifications are introduced by a set of controllable actuators (electric motors) installed on stiff tendons. Assuming the possibility of elongation and shortening of those members (stiff tendons), the aerostat volume and shape modifications are available. In Fig.1b, the nodal points of the supporting structure in an operational configuration are denoted by A'_i and B'_i. However, in the full 3D configuration the lengths modifications of vertical members affect the aerostat volume with the square exponent, while modifications of the horizontal ones affect it only linearly. The modifications of the aerostat shape can be used for volume corrections which affect the vertical and horizontal mobility (V-Mobility, H-stability).

3. MATHEMATICAL MODEL OF AEROSTAT MOTION

The numerical analyses presented in this paper consist of two parts. In the first part, we consider the motion of the aerostat and methods of controlling vertical and horizontal motion without the use of propulsion (horizontal motion of the aerostat under the influence of wind). For this purpose, a numerical model of the aerostat has been built to study the aerostat control and kinematics under atmospheric conditions (pressure, air density, temperature, gravity, wind direction and wind speed). The atmospheric conditions were approximated by an atmospheric

model according to NASA[i]. The data concerning wind directions and speeds at various altitudes were taken from FlyMeteo[ii] and are shown in Fig.2 in two views. The first view (Fig.2a) uses dual axes (one for wind speed, another one for wind direction), whereas the second view (Fig.2b) is oriented according to the directions of the World. Each pair of measurement data is aligned along the radial direction. An exemplary data for the highest altitude (about 16 km) is highlighted by the line *A–A'*.

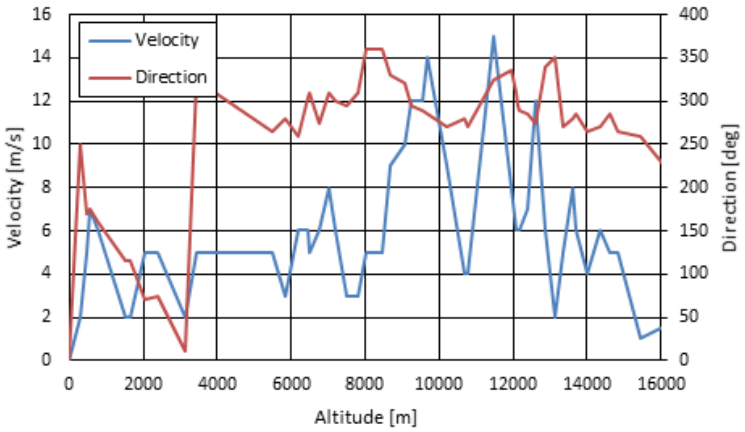

(a) Atmospheric data in the linear view.

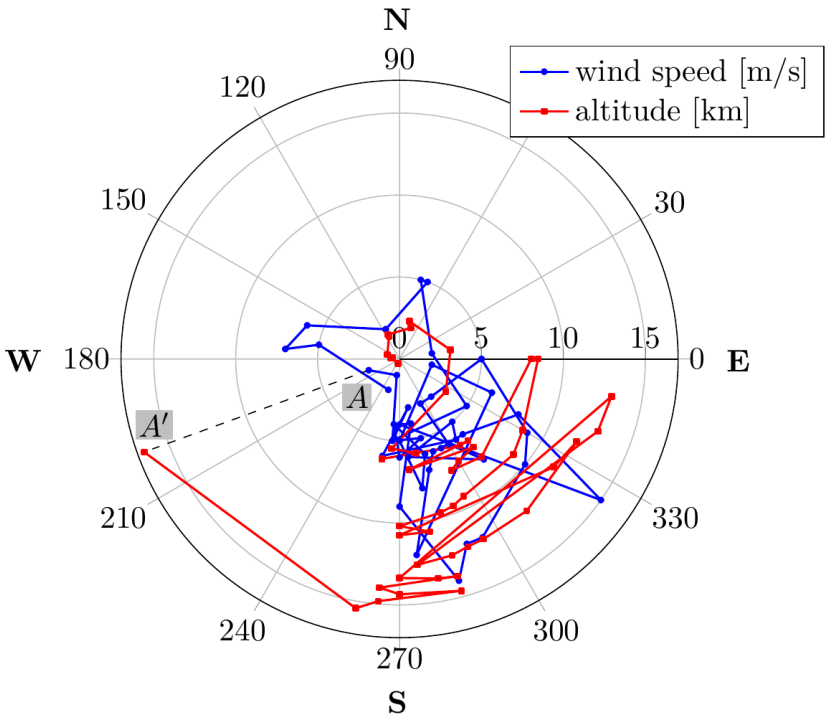

(b) Atmospheric data in the polar view.

Figure 2. Distribution of wind speed and direction for a sample location Praha-Libus (Czech Republic).

[i] Glenn Research Center. Earth Atmosphere Model Metric Units, (accesed on 21 June, 2021) https://www.grc.nasa.gov/www/K-12/airplane/atmosmet.html.
[ii] FlyMeteo, Wieter Pilot (accessed on 21 June, 2021), https://flymeteo.org/sounding/diag_p.php?p10&index=11520&termin=2021_06_20_00.

The motion of the aerostat in the atmosphere is described by the following system of equations:

$$m_t \frac{d^2x}{dt^2} = -Q_{dh} \cos\alpha \tag{1}$$

$$m_t \frac{d^2y}{dt^2} = -Q_{dh} \sin\alpha \tag{2}$$

$$m_t \frac{d^2h}{dt^2} = -Q_g + Q_b - Q_{dv} \tag{3}$$

where:

- x, y – spatial variables describing the movement of the aerostat in a horizontal plane (x – east, y – north),
- h – a spatial variable describing the movement of the aerostat in a vertical direction,
- α – an angle between the aerodynamic force exerted on the aerostat and the direction related with spatial variable x,
- m_t – total mass of the aerostat,
- Q_{dh} – aerodynamic force exerted by the wind in the horizontal direction,
- Q_{dv} – aerodynamic drag force in the vertical direction,
- Q_b – buoyancy force of the aerostat,
- Q_g – aerostat weight.

Mentioned above forces are determined as follows:

- the weight of the aerostat:

$$Q_g(h) = m_t g(h) \tag{4}$$

  where: $g(h)$ describes the value of the gravity in function of the altitude h,

- the buoyancy force of the aerostat:

$$Q_b(m_h, \varepsilon_t, h) = \rho_a(h)\, g(h) V(m_h, \varepsilon_t, h) \tag{5}$$

  where: $\rho_a(h)$ describes the air density at the altitude h, while $V(m_h, \varepsilon_t, h)$ describes the balloon volume as a function of the helium mass m_h in the aerostat balloon and $\varepsilon_t = \frac{l_t - l_t^0}{l_t^t}$ denotes the elongation of the stiff tendons with the actual length l_t and the initial length l_t^0.

- the aerodynamic drag force in the vertical direction:

$$Q_{dv}(m_h, \varepsilon_t, h) = \mathrm{sgn}(v_v)\, c_x(v_v, h)\, \rho_a(h) A_v(m_h, \varepsilon_t, h) \frac{v_v^2}{2} \tag{6}$$

  where: v_v denotes the vertical speed of the aerostat, $A_v(m_h, \varepsilon_t, h)$ is the cross-sectional area of the aerostat in the vertical direction, $c_x(v_v, h)$ is the drag coefficient in the vertical direction,

- the aerodynamic drag force in the horizontal direction:

$$Q_{dh}(m_h, \varepsilon_t, h) = sgn(v_h)\, c_x(v_h, h)\, \rho_a(h) A_h(m_h, \varepsilon_t, h) \frac{v_h^2}{2} \tag{7}$$

where: v_h denotes the horizontal speed of the aerostat, $A_h(m_h, \varepsilon_t, h)$ is the cross-sectional area of the aerostat in the horizontal direction, $c_x(v_v, h)$ is the drag coefficient in the horizontal direction.

In order to determine the value of the above forces it is necessary to know the volume occupied by the helium filling the aerostat balloon. The volume of helium depends on the mass of helium m_h inside the balloon, the properties of the envelope material and the atmospheric pressure outside the balloon.

In the case when the balloon volume V is smaller than the design value V_0 (with the balloon filled but without the imposing tensile stresses into the envelope), the pressure in the balloon p will be close to the atmospheric pressure p_a. If the balloon is fully inflated, the stretching of the balloon envelope has to be taken into account when determining the pressure value in the balloon. In addition, the control of the balloon volume below the volume V_0 can be conducted by changing the lengths of the tensegrity structure members (i.e. stiff tendons). Therefore, the volume V of the aerostat can be determined based on the system of equations:

$$V = \begin{cases} \frac{m_h R T_a(h)}{p_a(h)} & \text{for } V \le V_0 \text{ and } \varepsilon_t = 0 \\ \frac{V_0}{2k}\left(k - p_a(h) + \sqrt{\Delta}\right) & \text{for } V > V_0 \text{ and } \varepsilon_t = 0 \\ \hat{V}(\varepsilon_t, m_h, h) & \text{for } \varepsilon_t \neq 0 \end{cases} \tag{8}$$

The second relationship in Eq.(8) contains Δ which is a determinant of the equation:

$$\frac{k}{V_0}V^2 + (p_a - k)V - m_h R T_a = 0 \tag{9}$$

The above equation has one physical solution and results from the combination of the ideal gas law applied for helium inside the aerostat:

$$pV = m_h R T_a \tag{10}$$

and the equation defining the relationship between pressure p and the volume of the aerostat balloon V with the use of coefficient k defining elastic properties of the material of the aerostat envelope:

$$p - p_a(h) = k\left(\frac{V - V_0}{V_0}\right) \tag{11}$$

The value of the coefficient k can be determined numerically using simulation of the aerostat inflation based on Finite Element Method. Similarly, the relation between shortening of the tendons and volume of the aerostat can be obtained using corresponding FEM simulation of aerostat compression. The final dependence between mass of helium and aerostat volume, defined by Eq.8b, is presented in Fig.3a, whereas final dependence between tendons length reduction and aerostat volume, defined by Eq.8c, is shown in Fig.3b.

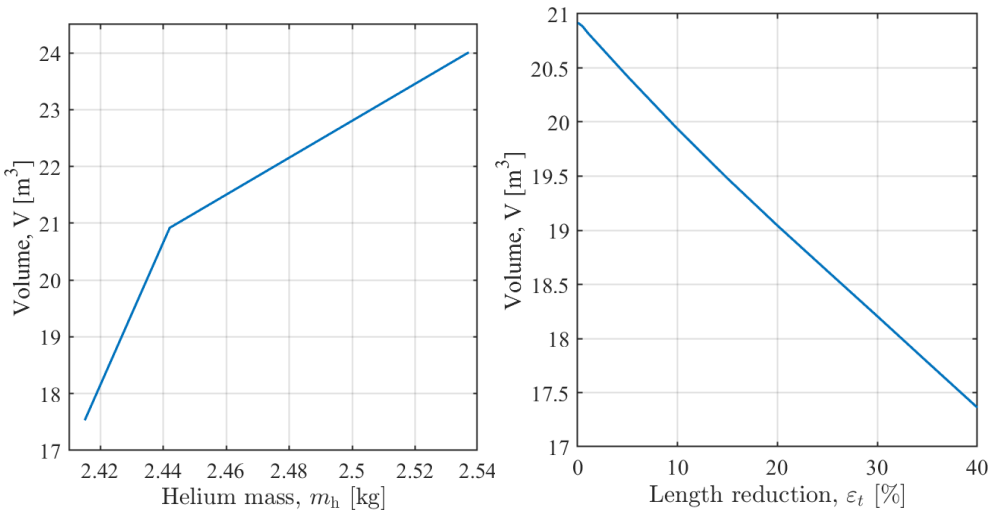

(a) Volume controlled by helium mass

(b) Volume controlled by tendons

Figure 3. Aerostat volume changes.

4. NUMERICAL SIMULATIONS

As mentioned in the Introduction, it is assumed that the aerostat can be transported to a selected point in the atmosphere in a folded position. Next, the aerostat can then be unfolded and filled with helium. Therefore, in the numerical model the simultaneous processes of filling the envelope and at the same time the free fall of the aerostat is taken into account. The analyses of the numerical results show that the process of unfolding the aerostat must be carried out as quickly as possible in order to prevent its deployment at high speed.

Using the mathematical model described above, it is possible to analyse the movement of the airship for different scenarios and two types of control:

- controlling the mass of helium, and
- controlling the length of tendons in the aerostat structure.

For example, it is possible to consider the scenario in which the mission in performed in such a way that aerostat position at the mission end is close to the position at the mission start. In such a case, the corresponding dynamic optimization problem is aimed at finding functions describing change of helium mass in time m_h^{opt} and tendons shortening in time $\varepsilon_t^{opt}(t)$, which minimize the difference between final horizontal position of the aerostat at arbitrary time instant t_{end} and its desired horizontal position (x_0, y_0):

$$\{m_h^{opt}(t), \varepsilon_t^{opt}(t)\} = \arg\min\left[\sqrt{[x(m_h(t), \varepsilon_t(t), t_{end}) - \mathrm{x}_0]^2 + [y(m_h(t), \varepsilon_t(t), t_{end}) - \mathrm{y}_0]^2}\right] \tag{12}$$

Solution of the above problem can be obtained by searching for the altitudes with winds of appropriate directions and using either helium mass control or tendons control in order to modify actual operational altitude of the aerostat, catch the suitable winds and use them for aerostat motion towards desired final position. Consequently, the following scenarios will be considered:

a) **Scenario 1** – this scenario corresponds to the execution of a sample standard mission consisting of steps:
   - Step 1 – ascending from $h_1 = 0$ m to $h_2 = 5$ km,

- Step 2 – maintaining the aerostat altitude at the level h_2 =5 km,
- Step 3 – descending to altitude h_3 =3.8 km at which volume $V = V_0$. In this step the decrease of the height takes place by decreasing the amount of helium in the aerostat balloon.
- Step 4 – maintaining the aerostat altitude at the level h_3,
- Step 5a – reducing the length of the stiff tendons by 34.4% and descending to the altitude $h_4 = 2$ km,
- Step 5b – maintaining the aerostat altitude at the level h_4,
- Step 6 – aerostat descending and landing at the level h_1 =0 m.

b) **Scenario 2** – this scenario corresponds to an almost identical mission as in Scenario 1, except that in Step 1 the aerostat is disembarked at an altitude h_2 and in Steps 5a and 5b the altitude is maintained in the range of 3.1-3.3 km so that it is possible to return to the initial position in the horizontal plane, but at h_0 level, due to wind effects.

In both scenarios, the control of the balloon volume and the ascending velocity is carried out both by the mass of helium control and the tendons length control. The control of vertical mobility is realized by tendons length control in the range of 2-3.8 km of the altitude, while outside this range by helium mass control. Tendon control outside this range is problematic because at a given helium mass it can lead to the formation of significant overpressures in the balloon which can lead to damage to the aerostat envelope. However, such a solution allows to operate between operational altitudes (e.g. 2-3.8 km) using only tendons and without changing the helium mass. Thus, it is possible to provide easier control of the aerostat altitude within the mentioned range. Additionally, volume change can be realized quickly which is difficult in the case of helium mass control.

In the Fig.4, the changes in the aerostat vertical motion control signals are presented. However, instead of the changes in the length of the tendons, the recalculated value of the decrease in the aerostat volume resulting from the assumed change in the length of the tendons is shown (maximum 39% for Scenario 1 and 11% for Scenario 2). The figure also presents a plot of the helium mass change in the aerostat balloon.

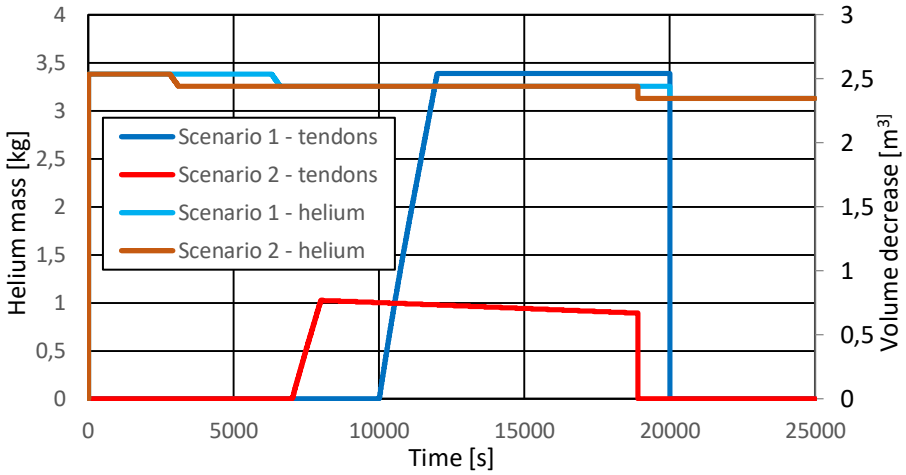

Figure 4. Variation of helium mass and balloon volume changes due to tendons control signals

Changes in control signals are accompanied by changes in the volume of the aerostat, which correspond to a change in balloon volume and therefore in the value of the buoyancy forces as well as ascending and descending velocities. The initial helium mass allows the aerostat to reach an altitude of 5 km in both scenarios - cf. Fig.5. Subsequently, the first decrease in helium mass

causes that the aerostat descends to an altitude of about 3.78 km. The next step of control consists of changing the length of the tendons. In the case of the maximum allowable shortening of the tendons, it is possible to reduce the height of the aerostat to an altitude of 2 km in Scenario 1. In Scenario 2, a different strategy of controlling the length of the tendons is adopted, which is aimed at obtaining a starting position in the horizontal plane. Therefore, it is necessary to search for altitudes at which the direction of the wind allows to return to the starting position without additional propulsion (cf. Fig.2). This is achieved by keeping the aerostat altitude in the range 3.1-3.3 km for some time. In Fig.6 the course of changes in the distance of the aerostat from the initial position is shown, while in Fig.7 its components in horizontal plane are presented. At the end of both scenarios, the second decrease in helium mass which leads to the landing of the aerostat and the end of the scenarios (Fig.4).

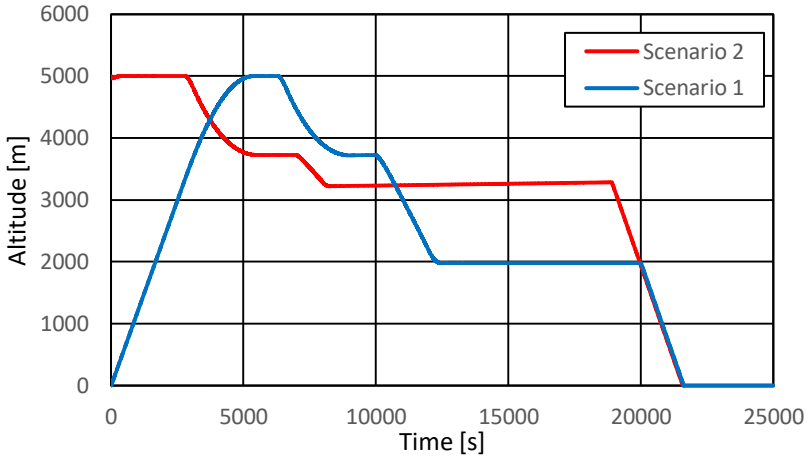

Figure 5. Change in aerostat altitude in Scenario 1 and 2.

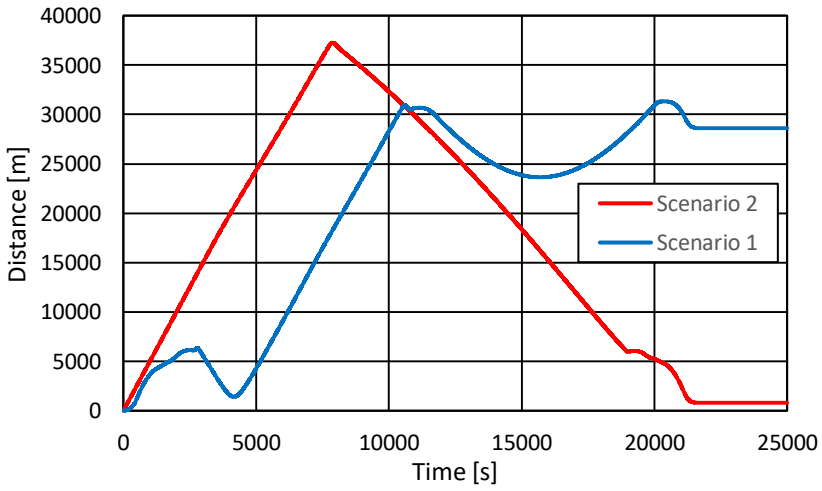

Fig. 6. Change in aerostat distance from initial horizontal position.

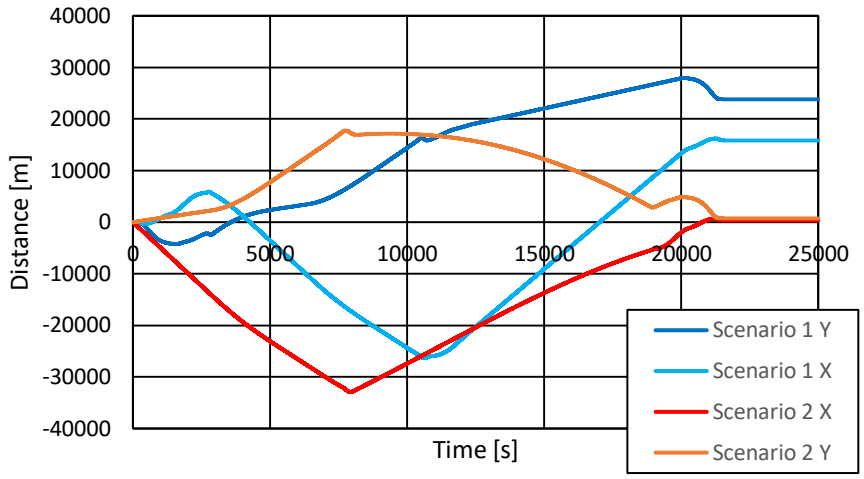

Figure 7. Change in aerostat distance components (direction X and Y) from initial horizontal position.

The obtained results indicate that in favourable atmospheric conditions it is possible to use the presented method of controlling the aerostat volume based on changing the length of the tensegrity structure tendons on which the balloon envelope is extracted. This approach enables both to control the change of the aerostat altitude and to maintain a certain horizontal position (circling around desired position) of the aerostat under favourable atmospheric conditions.

The durability of the aerostat envelope greatly depends on the gauge pressures inside the balloon. If the gauge pressure is too high during changes in helium mass or changes in tendon length, damage of the envelope may occur. Figure 8 shows the changes in the balloon gauge pressure (compared to atmospheric pressure at a given altitude) in both scenarios. Changes in helium mass and tendons lengths were limited in order to avoid obtaining a gauge pressure higher than 2150 Pa. Higher pressure can cause overloading of internal tensegrity structure and its damage. Also, attention should be paid to the fact that keeping a low value of a gauge pressure is favourable because it allows to increase resistance to wind gusts and the resulting undesirable changes in volume of the aerostat.

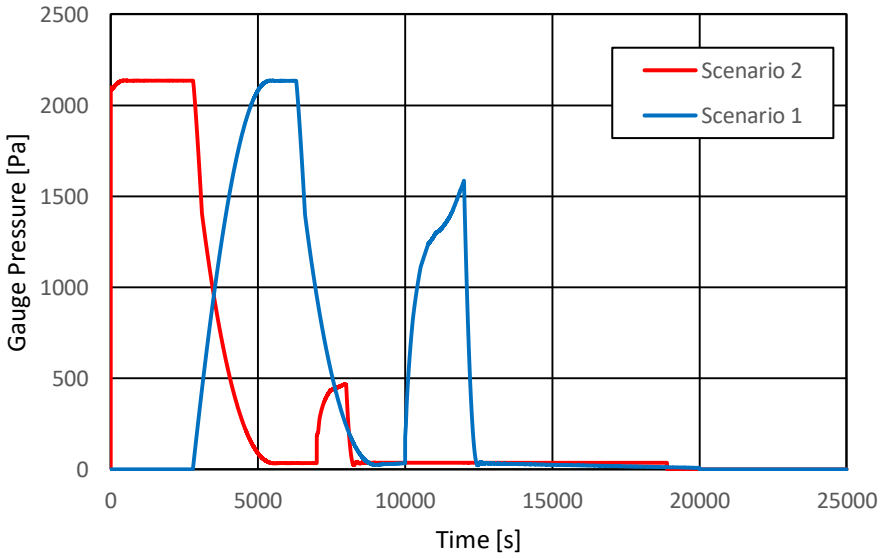

Figure 8. Change in the gauge pressure in the aerostat balloon.

5. FINITE ELEMENT STRENGTH ANALYSIS

The results of the numerical simulation based on above model of aerostat motion allow indicating the time instants in the aerostat motion where the structure is the most loaded. This is particularly visible in Step 2 at height h_2 where the gauge pressure has the highest value. In addition, the control of tendons length can also cause an increase in gauge pressure, what is visible in Step 5. Therefore, this section will present the results of the finite element analysis of the aerostat structure corresponding to the mentioned critical time instants.

For this purpose, a numerical model of the aerostat was created using Abaqus software. The ellipsoid-shaped aerostat has a length of 10 m (along the major axis) with circular cross-section (with respect to the vertical plane) and with the largest diameter of 2 m. It was assumed that the envelope is made of polyethylene (E=0.43 GPa) and has thickness of 50 μm. The supporting internal structure of the aerostat is composed of four separate modules of tensegrity structures. Each module is made of:

- carbon fibre bars (a pipe cross-section with outer diameter of 12 mm and wall thickness of 1mm),
- stiff tendons (circular cross-section with diameter of 3 mm, E=210 GPa) made of steel, and
- highly-elastic tendons (circular cross-section with diameter of 3.6 mm, E=0.05 GPa) made of a gum-like material.

For control of the stiff tendon lengths, the electric motors (retractors) are utilized and placed in each crossing of stiff tendons, as presented in Fig.9.

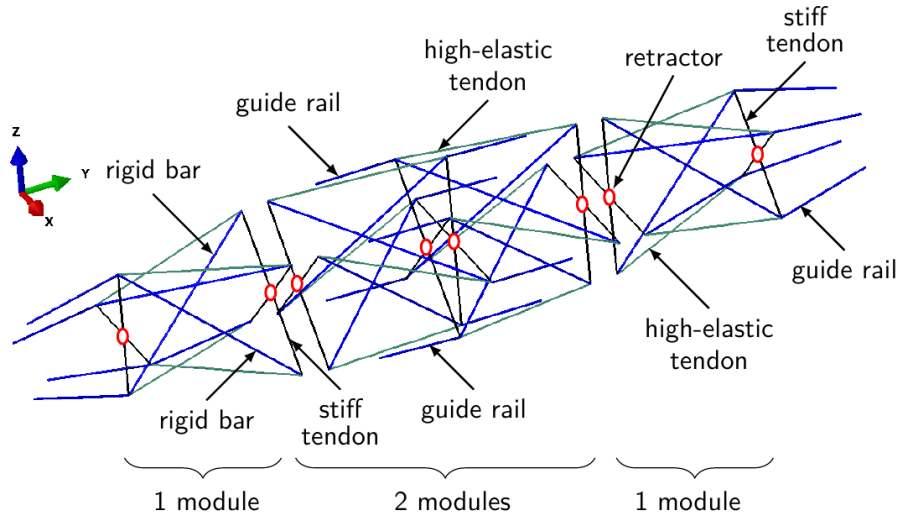

Figure 9. A scheme of the supporting structure.

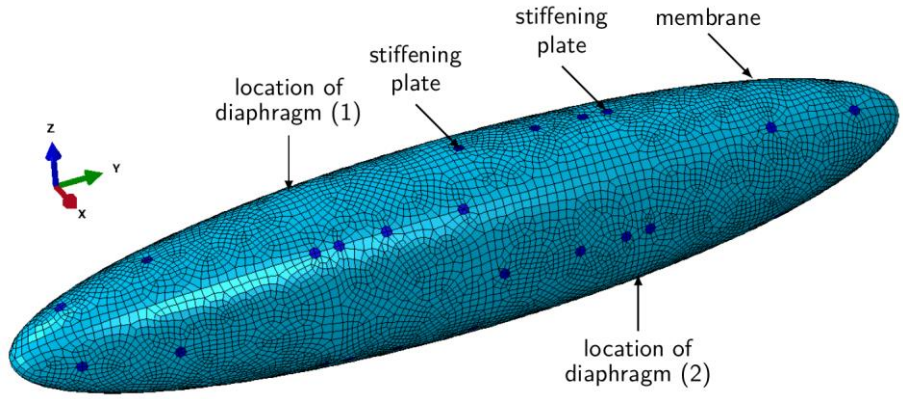

Figure 10. The supporting structure scheme of the aerostat.

The numerical model consisting of 13 811 finite elements (i.e. shell elements, membrane elements, truss elements and connectors) is shown in Fig.10. Total mass of the aerostat (including payload and helium) is equal to 17.709 kg. Each aerostat chamber was inflated proportionally and subjected to internal and external loadings (i.e. pressure, temperature) corresponding to the altitude of h_2=5 km. The model atmosphere was applied according to NASA's model.

Three aerostat loading cases are analysed as far as structural integrity is concerned:

i. an initial state with prestressed internal structure (σ_0 =2 MPa in high-elastic tendons) – aerostat ready for ascending (Step 1 valid for Scenario 1),
ii. the highest altitude of aerostat of 5 km (Step 2 valid for both scenarios), and
iii. the altitude of 2 km with partially released mass of helium and uniformly shortened tendons (about 34.4%) – Step 5b (valid for Scenario 1).

The computed stress distributions under aforementioned load conditions are presented in Fig.11. For the envelope, the equivalent von Mises stresses and for the internal structure, and the longitudinal stresses are visualised. In the initial state – case (i), small stress values are revealed in the envelope and in the internal structure. This is caused by initial stresses σ_0 introduced into the highly-elastic tendons. In the case (ii) – at the altitude of 5 km, the equivalent von Mises stresses in the envelope reach the level of 40 MPa, however in the stiffening plate they are much larger and reach about 65 MPa. In this state, the maximal longitudinal stresses in the tensegrity elements have the highest values of ca. 30 MPa.

A different stress distribution is revealed in the case (iii) when a small amount of helium is released and stiff tendons are shortened. The equivalent von Mises stresses in the envelope locally reach the values of ca. 20 MPa (in the stiffened plates about 40 MPa), whereas the internal structure is heavily loaded. The bars of the tensegrity structures are relatively slender and therefore can buckle. In order to ensure the integrity of the structure, it is important to apply appropriate structural material (e.g. carbon fibre) or increase its bending stiffness which, on the other hand, adversely influences the structural mass.

For comparison purposes, the total displacements corresponding to above discussed states are presented in Fig.12. Interestingly, for the considered cases the relatively small radial displacements of the envelope causes the largest state of stress in the envelope. However, the largest displacement for both internal structure and the envelope were obtained for the case (iii).

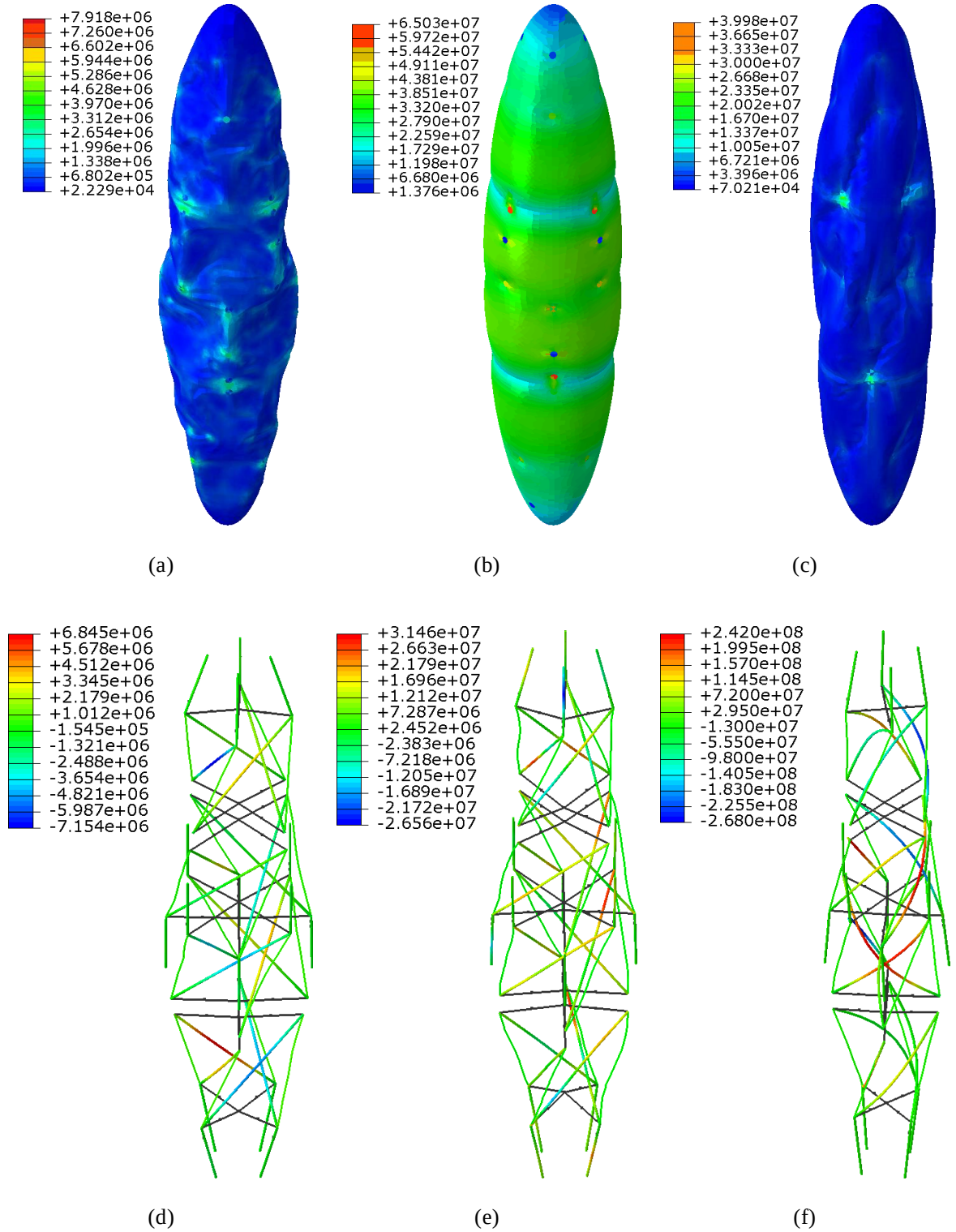

Figure 11. Distribution of stresses in the envelope (a)-(c) and internal structure (d)-(f) computed for: case (i) – first column, case (ii) – second column and case (iii) – third column
(no data in the greyed members – stiff tendons – modelled by connectors).

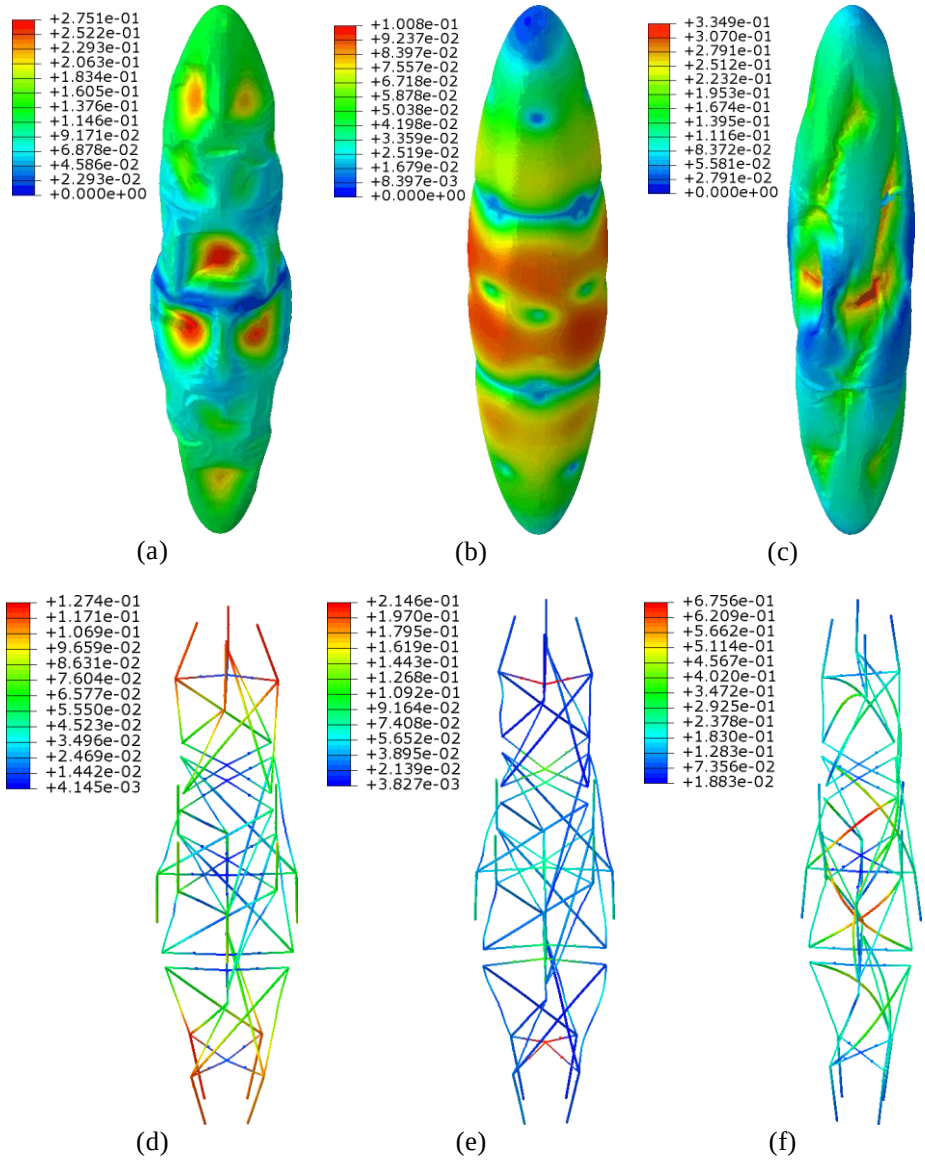

Figure 12. A map of total displacements in the envelope (a)-(c) and internal structure (d)-(f) computed for: case (i) – first column, case (ii) – second column and case (iii) – third column.

6. CONCLUSIONS

In this study, the aerostat internally supported by the tensegrity structure was presented and its hypothetical mission was analysed. The mission was considered in two scenarios. In the first one the aerostat starts form the ground level, whereas in the second one the aerostat is disembarked at initial non-zero altitude. The presented numerical model enables comparative analysis of both scenarios. It shows that it is possible to use internal tensegrity structure and apply tendons length control in order to ensure required aerostat altitude as well as to maintain horizontal position during favourable weather conditions. This type of control can significantly reduce the usage of energy during long aerostat missions. Moreover, it allows to adjust the altitude and horizontal position by limiting the amount of helium required during the aerostat operational range. On the other hand, the results of numerical analysis have shown that for a given distribution of wind speeds, a required

internal pressure can cause threats to envelope strength. Therefore, the structural strength analysis was also performed in order to ensure the aerostat structure integrity can be assured during the considered missions.

ACKNOWLEDGMENTS

The authors acknowledge the support of the National Centre for Research and Development and the National Science Centre, Poland, granted in the framework of the TANGO 4 programme (project TANGO-IV-C/0001/2019-00) and the project DEC-2017/25/B/ST8/01800 of the National Science Centre, Poland.

REFERENCES

[1] Recent Development Efforts for. Military Airships, The Congress of the United States, Congressional Budget Office (CBO), November 2011, https://fas.org/irp/program/collect/cbo-airship.pdf

[2] Saleh S., Weiliang HE., New design simulation for a high-altitude dual-balloon system to extend lifetime and improve floating performance, Chinese Journal of Aeronautics, Vol 31, No 5, pp. 1109-111, 2018.

[3] Loon.com. The Stratosphere: High Altitude, Higher Ambitions, https://loon.com/resources/content-library. [accessed on 21 June, 2021]

[4] Ghanmi A., Sokri A., Airships for military logistics heavy lift, Defence R&D Canada, Centre for Operational Research and Analysis, DRDC CORA TM 2010-011, 2010, https://cradpdf.drdc-rddc.gc.ca/PDFS/unc92/p532881.pdf.

[5] Future Aerostat and Airship Investment Decisions Drive Oversight and Coordination Needs, Report to the Subcommittee on Emerging Threats and Capabilities, Committee on Armed Services, U.S. Senate, GAO, 2012.

[6] Mizuta E., Akita D., Fuke H., IIjima I., Izutsu N., Kato Y., Kawada J., Matsuzaka Y., Nameki M., Nonaka N., Ohta S., Saito Y., Seo M., Takada A,. Tamura K., Toriumi M., Yamada K., Yamagami T., Yoshida T., Ichimura K., Kobayashi T., Development of a 2,5 um Plyethylene Film for the Hihgh Altitude Ballon, Trans JSASS Space tech Japan, Vol 7, No 26, 2009.

[7] H. Fuke, D. Akita, I. Iijima, N. Izutsu, Y. Kato, J. Kawada, Y. Matsuzaka, E. Mizuta, M. Namiki, N. Nonaka, S. Ohta, Y. Saito, M. Seo, A. Takada, K. Tamura, M. Toriumi, K. Yamada, T. Yamagami, T. Yoshida (2010), A new balloon base in Japan: Advances in Space Research, Vol. 45 (4), pp. 490-497

[8] Kumar B. S., Nagendra N., Ojha D. K., Peter G. S., Vasudevan R., Anand D., Kulkarni P. M., Reddy V. A., Development of Ultra-Thin Polyethylene Balloons for High Altitude Research upto Mesosphere. Journal of Astronomical Instrumentation. 03. 10.1142/S2251171714400029. 2014

[9] Gai M., Guglieri G., Lattanzi M. G., Lombardi A., Mana M., Masserano L., Musso I., Navone P., A Scientific Mission Based on a High Altitude Stratospheric Balloon, International Journal of Aerospace Sciences 2014, 3(1): 18-29

[10] Kayhan Ö., Hastaoglu M. A., Modeling of Stratospheric Balloon Using Transport Phenomena and Gas Compress–Release System, Journal of Thermophysics and Heat Transfer, Vol 28, No 3. 2014

[11] Saleh S., Weiliang HE., New design simulation for a high-altitude dual-balloon system to extend lifetime and improve floating performance, Chinese Journal of Aeronautics, Vol 31, No 5, 2018, pp. 1109-1118.